Cell Cycle 11:2, 384-394; January 15, 2012; © 2012 Landes Bioscience

Acm1 contributes to nuclear positioning by inhibiting Cdh1-substrate interactions

Juan S. Martinez, Hana Hall, Matthew D. Bartolowits and Mark C. Hall*

Department of Biochemistry and Center for Cancer Research; Purdue University; West Lafayette, IN USA

Key words: anaphase-promoting complex, pseudosubstrate, Cdh1, Hsl1, Acm1, cell cycle, mitosis

Abbreviations: APC, anaphase-promoting complex; Cdk, cyclin-dependent kinase; D box, destruction box; KEN box, lysine-glutamate-asparagine sequence; MS, mass spectrometry; GFP, green fluorescent protein; EGFP, enhanced green fluorescent protein; DAPI, 4,6-diamidino-2-phenylindole; PBS, phosphate-buffered saline; EDTA, ethylenediaminetetraacetic acid; PMSF, phenylmethylsulfonyl fluoride; G6PD, glucose-6-phosphate dehydrogenase; CEN, centromere sequence

The anaphase-promoting complex (APC) is tightly regulated during cell division, often by pseudosubstrate binding to its coactivators Cdh1 and Cdc20. Budding yeast Acm1 is a Cdh1 pseudosubstrate inhibitor whose biological function is unknown. We show here that cells lacking Acm1 have defects in nuclear positioning and spindle morphology during mitosis. However, Cdh1 substrates are not destabilized in the absence of Acm1, and expression of inactive Cdh1 mutants that retain substrate binding is sufficient for the *acm1* phenotype. We conclude that Acm1 is not required to inhibit APC^{Cdh1} activity, but rather prevents untimely Cdh1-substrate interactions. We further provide evidence suggesting that the substrate primarily responsible for the *acm1* phenotype is the bud neck-localized kinase, Hsl1. Our results imply that at least some coactivator-substrate interactions require regulation. Several unrelated APC pseudosubstrates have been identified in diverse eukaryotes, and their ability to simultaneously inhibit enzymatic activity and substrate binding may partly explain why this regulatory mechanism has been selected repeatedly during evolution.

Introduction

Regulated proteolysis directed by the anaphase-promoting complex (APC) is an essential component of the eukaryotic cell cycle.[1] APC is active primarily during mitosis and G_1 and targets numerous cell cycle regulatory proteins for ubiquitin-dependent degradation to ensure proper completion of mitosis and establishment of G_1.[2] Although APC is constitutively present, its activity is strictly regulated to ensure that substrates are destroyed at the appropriate time. Mitotic APC activity requires association with either Cdc20 or Cdh1, a pair of related WD40 repeat-containing proteins.[1] These coactivator subunits are primary targets for regulating APC activity.

Precise regulation of APC^{Cdh1} activity is critical for maintenance of genome stability and cancer avoidance. For example, Cdh1 is a haploinsufficient tumor suppressor in mice,[3] but, conversely, elevated Cdh1 expression has been correlated with malignancy in human tumors.[4] The ability of Cdh1 to activate APC is controlled by cyclin-dependent kinase (Cdk) phosphorylation, which inhibits association of Cdh1 with the core APC.[5,6] APC^{Cdh1} activity is thereby limited to the period of low Cdk activity from late mitosis until the end of G_1. However, other mechanisms also contribute to APC^{Cdh1} regulation, including inhibition by pseudosubstrate binding. Several unrelated APC pseudosubstrate inhibitors have been identified in diverse eukaryotes,[1] suggesting that they are an effective regulatory mechanism that independently evolved multiple times.

Substrates bind both to coactivators and the core APC, usually through one or more conserved degron sequences, such as the destruction box (D box) and the KEN box.[1] Pseudosubstrates use these degron sequences to bind tightly to coactivators or APC itself, somehow avoiding polyubiquitination and degradation and blocking binding of true substrates. What distinguishes a pseudosubstrate inhibitor from a substrate is poorly understood.

Budding yeast Acm1 is a Cdh1 pseudosubstrate inhibitor that uses conserved D and KEN boxes to tightly bind the Cdh1 WD40 domain.[7-10] Acm1 inhibits the ubiquitin ligase activity of APC^{Cdh1} in vitro and overexpression of Acm1 restores viability to strains expressing toxic levels of Cdh1, suggesting that it can inhibit APC^{Cdh1} activity in vivo. However, no cell cycle defects have been observed for strains lacking *ACM1*, whereas failure to inhibit Cdh1 by Cdk phosphorylation is lethal.[11] The broad conservation of *ACM1* within budding yeasts implies an important function. Since many APC^{Cdh1} substrates regulate or are components of the mitotic spindle, we predicted that loss of Acm1 might cause spindle defects due to premature Cdh1 substrate destabilization. Here, we report that yeast lacking Acm1 do exhibit defects in spindle morphology and position. Surprisingly

*Correspondence to: Mark C. Hall; Email: mchall@purdue.edu
Submitted: 06/28/11; Revised: 11/26/11; Accepted: 12/03/11
http://dx.doi.org/10.4161/cc.11.2.18944

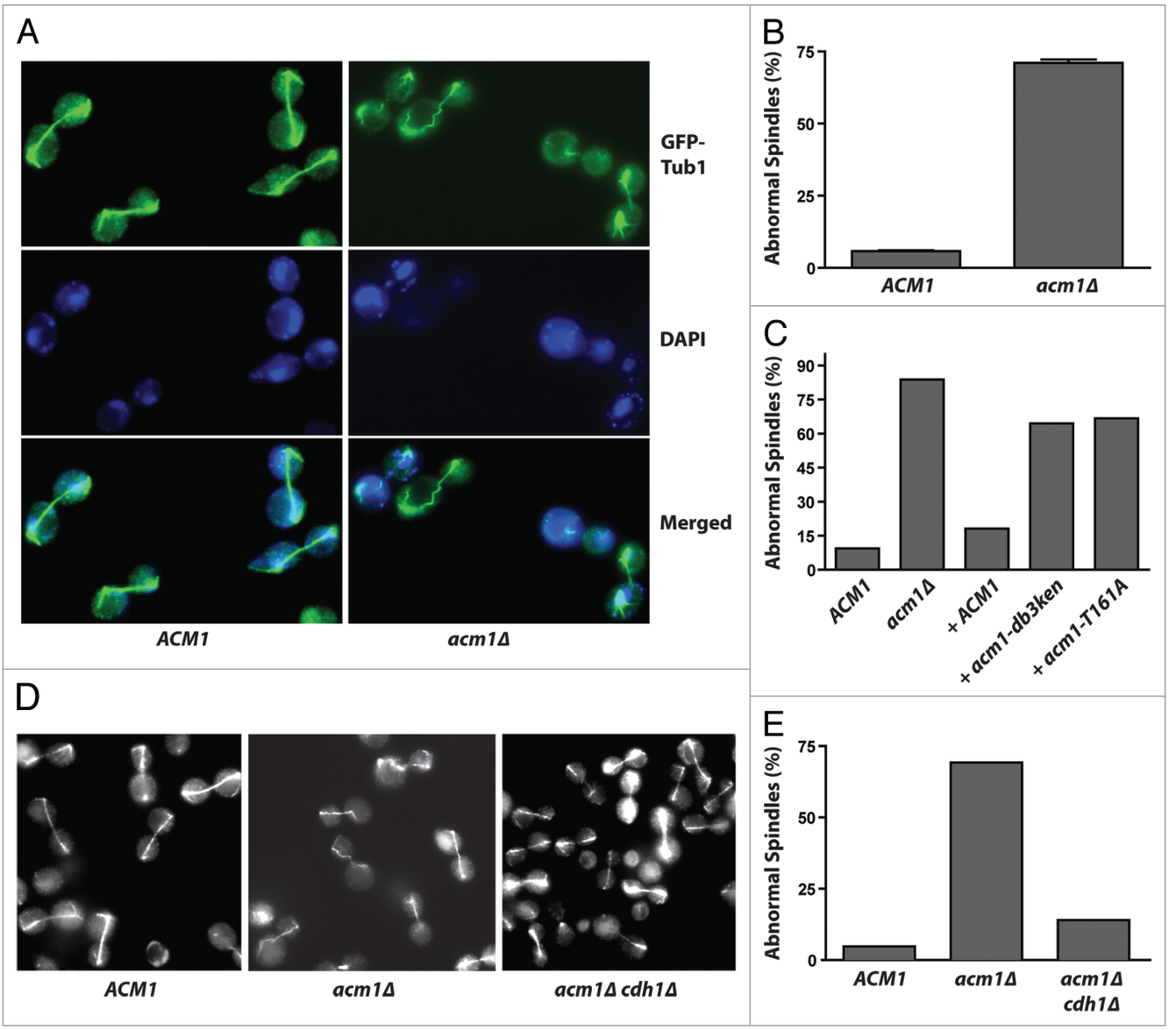

Figure 1. Cells lacking Acm1 have spindle defects when mitotic exit is delayed. (A) *cdc15-2 ACM1* and *cdc15-2 acm1*Δ cells expressing GFP-Tub1 were arrested at 37°C, fixed, treated with DAPI, and the spindle and DNA observed by fluorescence microscopy. (B) Quantification of abnormal spindles from (A) as described in Methods. Data are means of three experiments with standard deviations. (C) The indicated strains (*cdc15-2* background) were quantified as in (B) (n > 500 cells per strain). Centromeric plasmids expressing Acm1 variants from the *ACM1* promoter were used for complementation of *cdc15-2 acm1*Δ (+). (D) Same as (A), comparing *cdc15-2, cdc15-2 acm1*Δ and *cdc15-2 acm1*Δ *cdh1*Δ. (E) Quantification of abnormal spindles from (D) (n > 370 cells per strain).

though, these effects were independent of APC substrate degradation. The results suggest that an important function of Acm1 is to prevent untimely Cdh1-substrate interactions, and that Acm1 is dispensable for inhibition of APC enzymatic activity under normal conditions.

Results

To specifically test if *acm1*Δ cells exhibit spindle defects, we monitored spindle morphology in *cdc15-2* cells using GFP-tagged tubulin (GFP-Tub1) and fluorescence microscopy. The *cdc15-2* strain arrests in late anaphase at 37°C, and the mitotic spindle appeared as a straight line connecting the two segregated DNA masses in most large-budded cells. In contrast, spindles appeared broken or of abnormal morphology in the majority of *cdc15-2 acm1*Δ cells (**Fig. 1A and B**). The observed morphological abnormalities were diverse (**Fig. S1A**). Normal spindles were recovered upon reintroduction of wild-type Acm1, but the Acm1-db3/ken mutant, which has impaired Cdh1 binding due to loss of its pseudosubstrate motifs,[7] caused only slight recovery (**Figs. 1C and S1B**). Another mutant, Acm1-T161A, with a Thr to Ala point mutation in a Cdk phosphorylation site required for

binding of the 14-3-3 proteins Bmh1 and Bmh2 [12] also failed to significantly rescue the *acm1*Δ defect. Analysis of cells by confocal microscopy revealed that many of the apparently broken spindles are actually probably intact but of abnormal and nonlinear morphology, resulting in sections outside the focal plane (**Fig. S1C**). Due to the complexity of observed spindle structures, we refer to the phenotype generally as a spindle morphology defect. Because the effect was most readily quantitated from conventional epifluorescence images such as those in **Figure 1**, we report results from this approach for the remainder of the experiments.

Spindles appeared mostly normal in *acm1*Δ *cdh1*Δ cells (**Fig. 1D and E**), although we noticed that *cdh1*Δ alone causes a mild spindle defect (not shown). Thus, the phenotype is related to Acm1's interaction with Cdh1 and not to an independent function. S-phase and metaphase spindles appeared similar in *ACM1* and *acm1*Δ cells, suggesting that the effect was unique to elongated anaphase spindles (**Fig. S1D**).

Spindle abnormalities are often indicative of an imbalance in forces exerted on the cytoplasmic and spindle microtubules that are responsible for positioning the nucleus and controlling spindle elongation.[13] Consequently, conditions that impair the cytoplasmic microtubule system, such as absence of Dyn1, a subunit of cytoplasmic dynein, lead to improper nuclear and spindle positioning. In *dyn1*Δ cells, this is manifested as nuclear division exclusively within the mother.[14] Since this phenotype is easy to observe in *dyn1*Δ strains, we first tested if Acm1 affects nuclear positioning by measuring the frequency of binucleate mother cells in asynchronous *dyn1*Δ and *dyn1*Δ *acm1*Δ cultures. Surprisingly, there was a dramatic increase in the percentage of large-budded *dyn1*Δ *acm1*Δ cells with two nuclei in the mother compared with *dyn1*Δ alone (**Fig. 2A and B**). Given the magnitude of the effect, we next tested *acm1*Δ alone for a binucleate mother phenotype (**Fig. 2C**). A small but highly significant increase in binucleate mother cells was observed both at 12°C and in a *cdc15-2* background after arrest at 37°C. The nuclear position defect in *acm1*Δ cells was complemented by wild-type Acm1 but not the Acm1-db3/ken or Acm1-T161A mutants (**Fig. 2D and E**). Thus, as with spindle morphology, this phenotype apparently depends on Acm1 interaction with Cdh1 and the 14-3-3 proteins Bmh1 and Bmh2. We could not directly test dependency on Cdh1 in this experiment, as we found that *cdh1*Δ cells also exhibit a nuclear position defect (**Fig. S2**), something that has been noticed before and attributed to uncoupling of bud formation and mitosis due to mis-regulated mitotic kinase activity.[15] In addition to binucleate mother cells, we also observed a statistically significant increase in multinucleate cells (> 2 nuclei) in *acm1*Δ strains, suggesting that a fraction of mis-positioned spindles escape correction prior to cytokinesis in the absence of Acm1 (**Fig. 2F–H**).

A logical explanation for the *acm1*Δ phenotypes is premature degradation of APC^{Cdh1} substrates. We compared immunoblot profiles of several Cdh1 substrates from synchronized *cdc15-2* and *cdc15-2 acm1*Δ cultures released from early cell cycle arrests at 37°C (**Fig. 3**). At the *cdc15-2* arrest point, Cdh1 substrates were stable as expected, because Cdh1 is normally inactive under these conditions. Surprisingly, we saw no evidence for destabilization of any of the Cdh1 substrates tested in the *cdc15-2 acm1*Δ strain, including substrates associated with spindle function and stability, such as Ase1,[17] Fin1,[18] Clb2 [19] and Cdc5 [20] as well as the cytoplasmic substrates Hsl1 [21] and Cik1.[16] Conditions were identical to those under which we observed the spindle defects in **Figure 1**. Acm1 has been shown to block the binding of Clb2 and Hsl1 to Cdh1,[7,9,10,22] and ubiquitination of several of these substrates by APC^{Cdh1} is inhibited by Acm1 in vitro.[7,9,22] However, our results here argue that Acm1 is not required for APC^{Cdh1} inhibition in vivo, even in anaphase, when Cdk activity has been lowered by cyclin degradation.[23]

It was previously suggested that Acm1's pseudosubstrate properties could be important for preventing inappropriate Cdh1-substrate interactions.[8,9] To distinguish between dependence of the *acm1*Δ phenotypes on APC^{Cdh1} activity vs. Cdh1 substrate binding, we took advantage of previously characterized Cdh1 mutants. Cdh1 contains two separate sequence elements, the C box and the IR motif, required for binding to and activating the core APC.[24,25] Mutation of these sequences eliminates APC^{Cdh1} activity[24,26] but does not affect substrate binding.[27] We integrated wild-type *CDH1* or the mutant *cdh1-C/IR* allele containing a C-box mutation (R56D) and IR deletion under control of the *CDH1* promoter in a *cdc15-2 acm1*Δ *cdh1*Δ strain and examined spindle morphology as described above. Abnormal spindle morphology was minimal in the control strain but was equally prominent in cells expressing wild-type Cdh1 or the Cdh1-C/IR mutant (**Fig. 4A and B**). The isolated WD40 domain of Cdh1 is sufficient for Acm1 binding[7] and contains the binding site for D box-containing substrates[26,28] but lacks the C box required for APC activation. We also expressed the WD40 domain of Cdh1 without the terminal IR sequence (Cdh1-WD) in *cdc15-2 acm1*Δ *cdh1*Δ cells, and found that it too resulted in abnormal spindle morphology, similar to that observed for wild-type Cdh1 (**Fig. 4A and B**). These results demonstrate that the *acm1*Δ phenotypes are independent of APC^{Cdh1} activity.

A binding site for substrate D boxes was previously mapped on the human Cdh1 WD40 domain, and a mutant (Cdh1-D12) containing several substitutions at this site strongly reduced substrate binding and ubiquitination in vitro.[26] Mutation of the homologous residues in budding yeast Cdh1 also disrupted substrate binding[28] and prevented Clb2 proteolysis in vivo (**Fig. 4E**). We integrated the full-length *cdh1-D12* allele into our *cdc15-2 acm1*Δ *cdh1*Δ strain and found that, unlike wild-type Cdh1, the Cdh1-D12 mutant did not cause a spindle morphology defect (**Fig. 4C and D**). Taken together, the results thus far strongly suggest that the *acm1*Δ phenotypes are dependent only on binding of Cdh1 to one or more substrates via the D-box receptor site on its WD40 domain.

To reveal potential Cdh1 targets responsible for the observed phenotypes, we used mass spectrometry (MS) to identify Cdh1 binding partners in cells lacking Acm1. Acm1 was first identified using this approach, as it forms a stable stoichiometric complex with Cdh1 and Bmh1/Bmh2 during the period of high Cdk activity from G_1/S until late mitosis.[10,22] We reasoned that additional tight binding partners of the Cdh1 D-box receptor

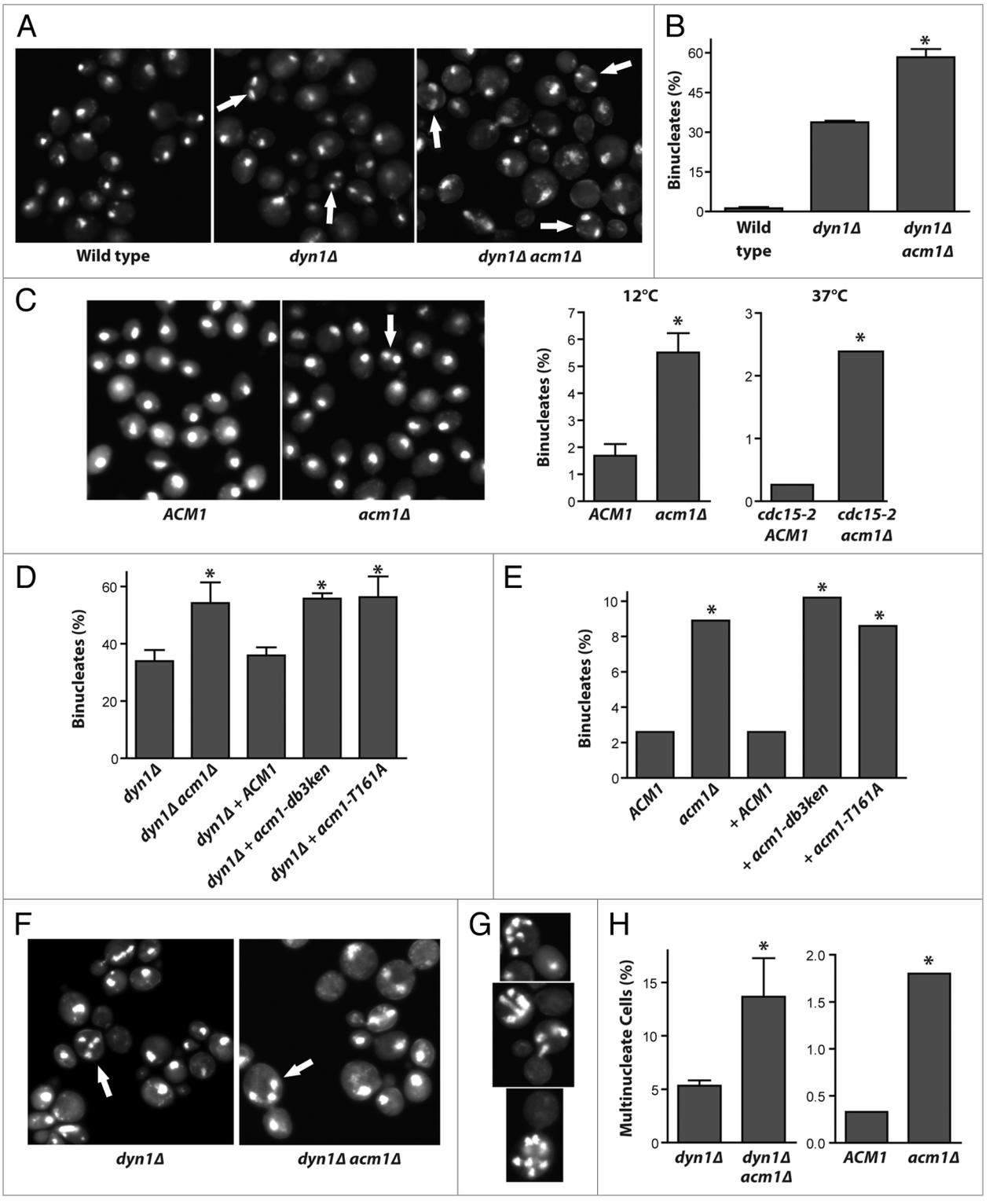

Figure 2. Cells lacking Acm1 display a nuclear position defect. (A) The indicated strains (BY4741 background) were grown at 12°C, fixed, treated with DAPI and visualized by fluorescence microscopy. Arrows show examples of binucleate mother cells (DNA segregation within the mother). (B) Quantification of binucleate mothers from (A) as described in Methods. *$p < 10^{-6}$ from chi square test compared with *dyn1*Δ. (C) Same as (A and B) for *ACM1* and *acm1*Δ strains either at 12°C or in *cdc15-2* background arrested at 37°C. Images are from the experiment at 12°C. Binucleate mothers (white arrow) were quantified as described in Methods. (D) *dyn1*Δ *acm1*Δ cells were complemented with a CEN plasmid expressing either *ACM1*, *acm1-db3/ken* or *acm1-T161A* alleles from the *ACM1* promoter (+), and nuclear position was quantified as in (B). (E) Complementation of *acm1*Δ cells as in (D). (F) Multinucleate cells (white arrows) in the indicated strains were detected as in (A). (G) Additional examples of multinucleate *dyn1*Δ *acm1*Δ cells from (F). (H) Quantification of cells with more than two nuclei from (F). For all parts with quantitative analyses, n > 550 cells per strain. When present, error bars are standard deviations of the mean of three experiments. Asterisks (*) in (C–E and H), $p < 10^{-6}$ from chi square test compared with control (first bar).

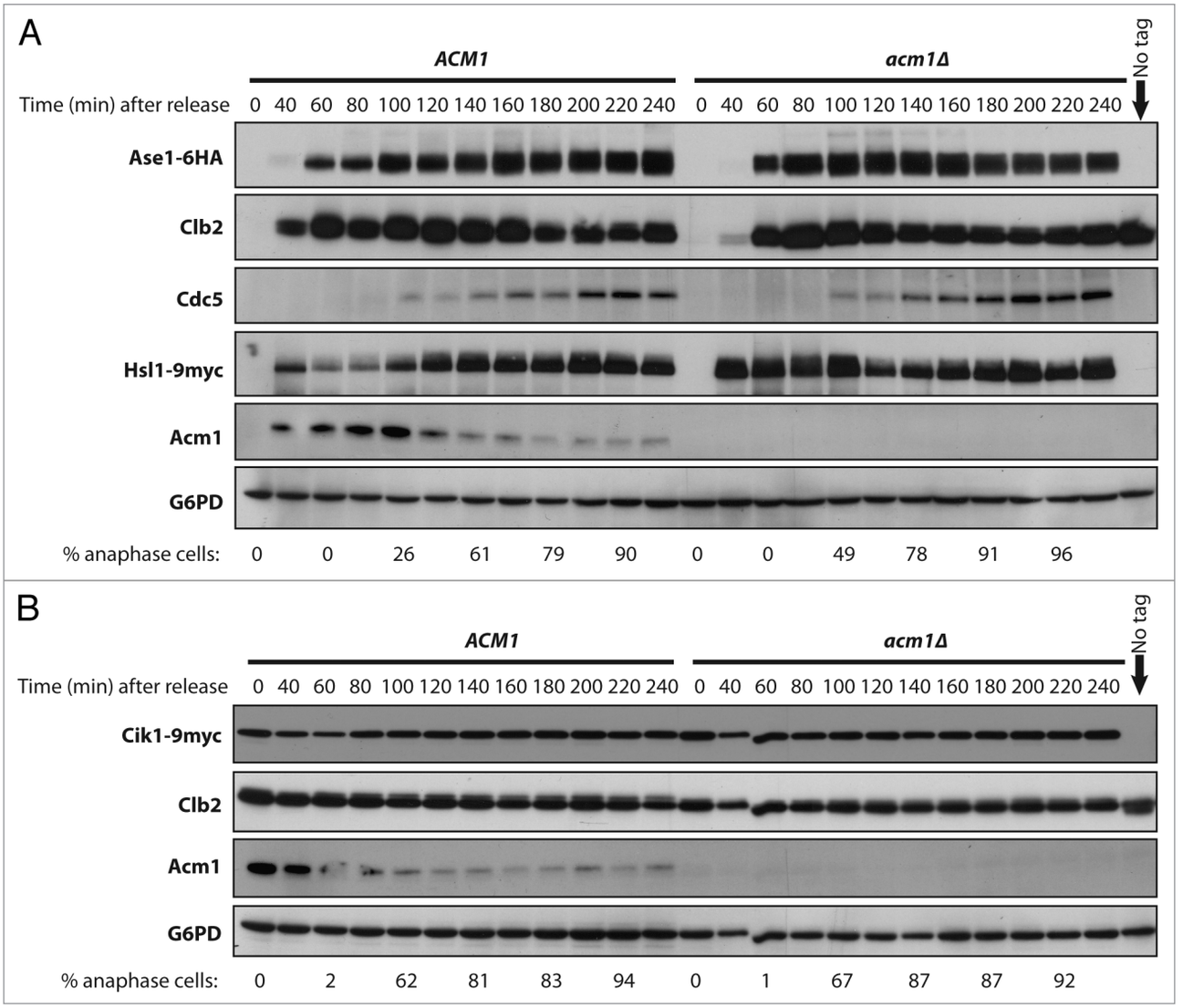

Figure 3. Lack of Acm1 does not destabilize Cdh1 substrates. (A) Levels of Cdh1 substrates at the indicated timepoints after release of *cdc15-2 ACM1* and *cdc15-2 acm1*Δ cultures from an α factor-induced G_1 arrest were compared by immunoblotting. The synchronized cells were released at restrictive temperature (37°C) to cause arrest in late anaphase. Note that all blots (and the anaphase quantification) are from the same experiment using *ASE1–6HA* strains except the Hsl1 blot, which was from an identical experiment using *HSL1–9myc* strains. Similar results were also obtained for Fin1–6HA (not shown). Anaphase arrest was confirmed by monitoring DNA segregation (DAPI). G6PD, loading control. (B) Same as (A), except strains with *CIK1–9myc* were released from S phase arrest at 37°C, because α factor arrest in G_1 results in expression of a truncated isoform that is resistant to APC.[16]

site might be revealed using the same approach in an *acm1*Δ background. We affinity purified both the Cdh1-C/IR mutant and the isolated Cdh1 WD40 domain from cell extracts under physiological conditions after expression from the *GAL1* promoter in *acm1*Δ *cdh1*Δ cells and separated the proteins by SDS-PAGE (**Fig. S3**). Co-purifying proteins were identified by MS. The Cdh1-C/IR mutant was used to prevent APC-mediated degradation of interacting substrates, and the WD40 domain was used to enrich specifically for proteins interacting with the D-box (and Acm1) binding site on Cdh1. Identical preparations from strains lacking the fusion constructs were used as controls for specificity. Although numerous specific interacting proteins were identified in the Cdh1-C/IR and the WD40 domain preparations (**Tables S3 and S4**), only two were known Cdh1 substrates, suggesting that most substrates do not associate with Cdh1 stably enough to remain bound throughout the purification procedure. Hsl1 was the only known substrate, and one of only two proteins total, that were common binding partners of both Cdh1-C/IR and the Cdh1 WD40 domain. We confirmed by immunoblot that the mitotic cyclin Clb2 also specifically interacted with both Cdh1-C/IR and the WD40 proteins (not shown); however, it was apparently not abundant enough for detection by MS.

Hsl1 seemed a likely culprit for the *acm1*Δ phenotypes. First, Hsl1 is a well-characterized APC^{Cdh1} substrate[21] with conserved D-box and KEN-box motifs that interact with the substrate receptor site on the Cdh1 WD40 domain.[27-29] Acm1 also binds this site and was previously shown to competitively inhibit Hsl1

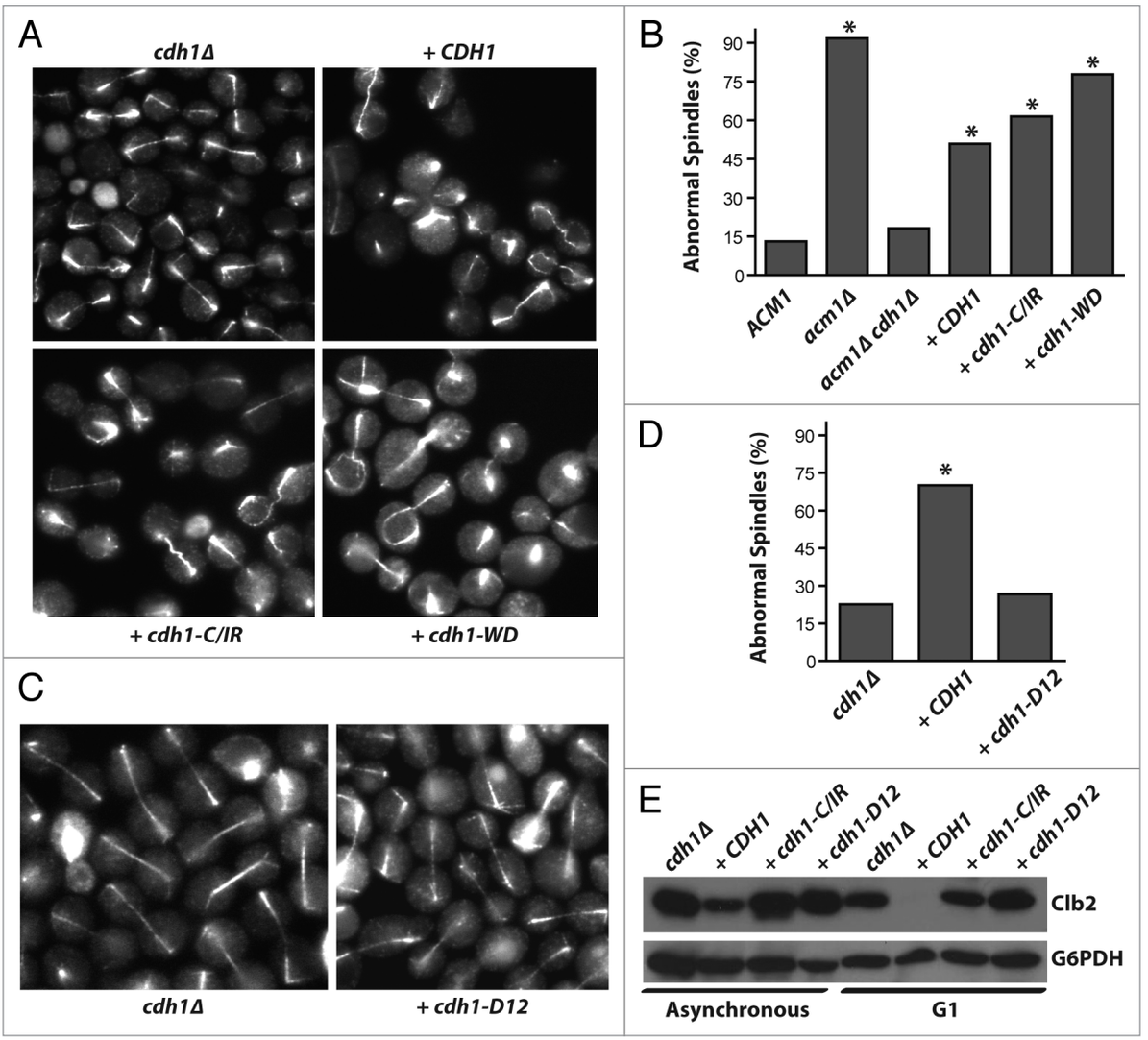

Figure 4. Spindle defects in *acm1*Δ are independent of APC^{Cdh1} activity. (A) GFP-Tub1 was monitored by fluorescence microscopy in *cdc15-2 acm1*Δ *cdh1*Δ cells (*cdh1*Δ) complemented with integrating plasmids expressing 3FLAG-Cdh1 or 3FLAG-Cdh1-C/IR from the *CDH1* promoter or a CEN plasmid expressing 3FLAG-Cdh1-WD from the *ADH* promoter (+) and arrested at 37°C. (B) Quantification of abnormal spindles from (A) as described in Methods. (C) Same as (A), with complementation by an integrating plasmid expressing 3FLAG-Cdh1-D12 from the *CDH1* promoter. (D) Quantification of (C), including complementation by wild-type Cdh1. For (B and D), n > 400 cells per strain. *$p < 10^{-6}$ from chi square test compared with control (first bar). (E) Clb2 levels in asynchronous or G_1-arrested cells of the indicated strains used in (A and C) were monitored by immunoblot as a measure of APC^{Cdh1} activity. G6PD, loading control.

association with Cdh1 in vivo and in vitro.[7,9,10] Moreover, Hsl1 localizes to the yeast bud neck,[30] and we previously observed that Cdh1 preferentially localizes to the bud neck in the absence of Acm1.[10] The bud neck is an important interaction site for cytoplasmic microtubules, as they act to position and align the nucleus.[13] Thus, we speculated that Hsl1 recruits Cdh1 to the bud neck, and that Acm1 prevents this interaction until the appropriate time in late mitosis.

To initially test this idea, we monitored the bud neck localization of Cdh1-EGFP fusion proteins. First, we examined Cdh1-EGFP localization to the bud neck in *cdc15-2* cells arrested in late anaphase at 37°C. As seen previously at other cell cycle stages,[10] Cdh1 preferentially localizes to the bud neck in the absence of Acm1, and the extent of Cdh1 localization to the bud neck was sensitive to the level of Acm1 (**Fig. 5A and B**). This confirms that Cdh1 localization to the bud neck is controlled by Acm1 at the same cell cycle stage during which we observe spindle and nuclear position defects. Next, we compared localization of wild-type Cdh1 and the Cdh1-D12 mutant that alleviates the *acm1*Δ phenotype (**Fig. 4**) and has impaired Hsl1 binding capacity.[28] In asynchronous, S phase-arrested and late anaphase-arrested *cdc15-2 acm1*Δ *cdh1*Δ cultures, wild-type Cdh1 was readily detected at the bud neck in the majority of budded cells (**Fig. 5C** and not shown). In contrast, fluorescence signal for the Cdh1-D12 mutant was never observed at the bud neck under any conditions despite the mutant protein being expressed at the same level as wild-type Cdh1 (**Fig. 5D**). We conclude that a D box-dependent interaction is required for

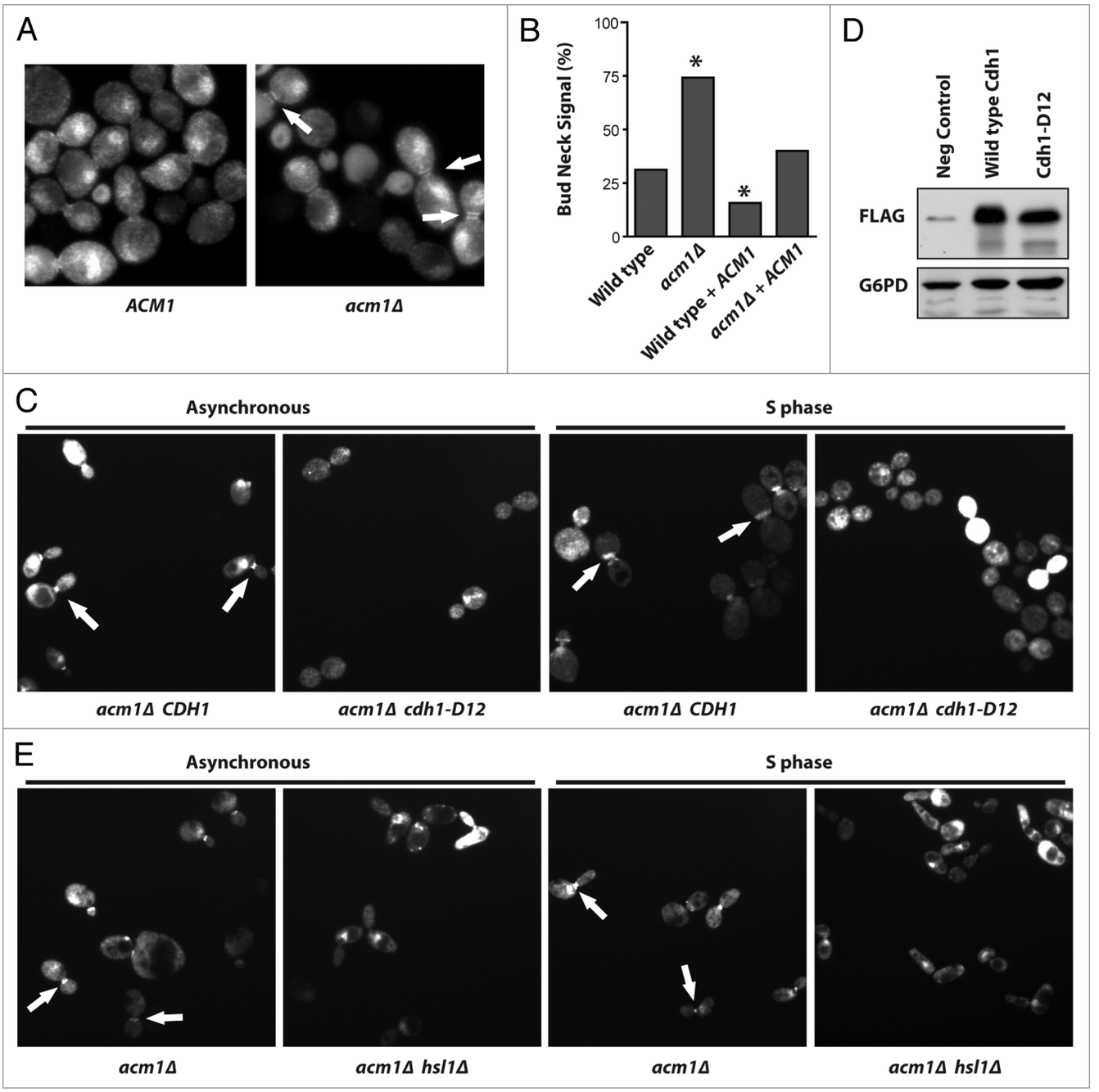

Figure 5. *acm1*Δ phenotypes correlate with Cdh1-Hsl1 interaction and localization to the bud neck. (A) Representative fields of view showing localization of 3FLAG-Cdh1-EGFP fusion protein expressed from P_{ADH1} on a CEN plasmid in *cdc15-2 cdh1*Δ (left) and *cdc15-2 cdh1*Δ *acm1*Δ (right) cells arrested at 37°C for 3 h prior to microscopy. Arrowheads indicate examples of bud neck localization. (B) The percentage of large-budded cells containing detectable bud neck staining from the experiment in (A) was quantified. In addition, localization was quantified after addition of a plasmid expressing *ACM1* from its natural promoter (+*ACM1*). A minimum of 140 cells were counted per strain. *p < 0.0005 in chi square analysis compared with *ACM1* (wild type, first bar). (C) Localization of wild-type Cdh1 and the Cdh1-D12 mutant as described in (A) in asynchronously growing cells and cells arrested in S phase with hydroxyurea. (D) Expression of 3FLAG-Cdh1-EGFP (wild type) and 3FLAG-Cdh1-D12-EGFP were compared in the asynchronous cultures used for (C) by immunoblot with anti-FLAG antibody. G6PD is a loading control. The negative control sample (Neg Control) is from *cdc15-2 cdh1*Δ *acm1*Δ cells without an expression plasmid and contains a faint non-specific band commonly observed in our FLAG immunoblots that co-migrates with the FLAG-Cdh1-EGFP fusion protein. (E) Representative fields of view showing localization of 3FLAG-Cdh1-EGFP expressed from P_{ADH1} on a CEN plasmid in *acm1*Δ and *acm1*Δ *hsl1*Δ cells either growing asynchronously or arrested in S phase with hydroxyurea. Arrowheads highlight examples of bud neck localization.

recruitment of Cdh1 to the bud neck, and that Acm1 binding prevents this localization.

To directly test if Hsl1 recruits Cdh1 to the bud neck, we compared Cdh1-EGFP localization in *acm1*Δ *HSL1* and *acm1*Δ *hsl1*Δ strains (**Fig. 5E**). Cdh1-EGFP fluorescence signal was detected at the bud neck in *acm1*Δ *HSL1* cells, as expected. Although *acm1*Δ *hsl1*Δ cells exhibit an irregular morphology typically involving hyperpolarized growth, Cdh1-EGFP fluorescence signal was nonetheless consistently absent from the bud neck. Thus, Hsl1 is required for Cdh1 bud neck localization.

To test if the Hsl1-Cdh1 interaction is related to the observed *acm1*Δ phenotypes, we deleted *HSL1*, integrated either *3FLAG-HSL1* or a *3FLAG-hsl1-mdb/mkb* allele containing D-box and KEN-box mutations that prevent Cdh1 binding[29] under control of the weakened *GALL* promoter and compared the severity of the spindle and nuclear position defects in galactose medium. We reasoned that if the Hsl1-Cdh1 interaction were responsible for the phenotypes, they might be rescued by specifically preventing the interaction. Unfortunately, the modest overexpression of Hsl1 in the *cdc15-2 acm1*Δ background caused morphogical abnormalities that prevented reliable scoring of spindle structure (not shown). In the *acm1*Δ *dyn1*Δ background, cells were very sick and also morphologically abnormal at the 12°C growth temperature used for assaying the nuclear division defect. However, we found that we could effectively score nuclear position at 18°C in these cells. We counted both anaphase cells and total cells to account for potential cell cycle distribution differences. In both cases, the frequency of binucleate/multinucleate cells expressing the Hsl1-mdb/mkb mutant was significantly lower than that of cells expressing wild-type Hsl1 [10% vs. 16% for anaphase cells ($p < 10^{-6}$, minimum 800 cells counted) and 2% vs. 4% for total cells ($p < 10^{-6}$, minimum 5,000 cells counted)]. These differences were highly reproducible in independent experiments. The frequency of binucleate/multinucleate cells in the control *dyn1*Δ strain was 11% (anaphase cells) and 2% (total cells), suggesting that preventing the Hsl1-Cdh1 interaction largely rescued the nuclear position defect caused by absence of Acm1.

Discussion

We have described the first biological function for budding yeast Acm1. The mitotic defects in nuclear positioning and spindle morphology are both consistent with misregulation of the forces acting on the cytoplasmic and/or nuclear microtubule systems. These phenotypes were dependent on Acm1 interaction with Cdh1 and the 14-3-3 proteins Bmh1 and Bmh2. They were also dependent on Cdh1 and the D-box receptor site on the Cdh1 WD40 domain but were surprisingly independent of APC^{Cdh1} activity. We conclude that a primary biological function of Acm1 is to prevent inappropriate interactions between Cdh1 and one or more substrates involved in regulating nuclear position and spindle elongation during the cell cycle period in which APC^{Cdh1} is kept inactive. Our results implicate the bud neck-localized Hsl1 kinase as a key substrate whose interaction with Cdh1 in the absence of Acm1 perturbs normal nuclear and spindle positioning.

Hsl1 was the only Cdh1 substrate that we found stably associated with the Cdh1 WD40 domain in the absence of Acm1. The ability of Acm1 to competitively inhibit the Cdh1-Hsl1 interaction is well-established;[7,9,10,28] however, it was surprising that no other Cdh1-substrate interactions were reproducibly detected in our MS experiments using overexpressed Cdh1-C/IR and Cdh1-WD40. This implies that Hsl1 is capable of an unusually high affinity interaction with the substrate receptor site on the Cdh1 WD40 domain compared with other substrates. The Cdh1-D12 mutant containing point mutations in the D-box binding site,[26] which fails to bind Hsl1 [28] and alleviates the *acm1*Δ phenotype, also fails to localize to the bud neck. This suggests that interaction with a D box-containing substrate is required to recruit Cdh1 to the bud neck in the absence of Acm1 and is consistent with a prior study that noted lack of bud neck localization for a different Cdh1 mutant with impaired substrate binding.[31] Furthermore, Cdh1 does not localize to the bud neck in cells lacking Hsl1. Finally, under defined growth conditions, we found that replacing wild-type Hsl1 with a mutant specifically defective in binding Cdh1 rescued the nuclear position defect in *acm1*Δ cells. Taken together, our results suggest that (1) Hsl1 recruits Cdh1 to the bud neck through a direct physical interaction; (2) Acm1 acts to prevent this interaction and localization, and (3) the inappropriate recruitment of Cdh1 to the bud neck by Hsl1 somehow perturbs nuclear position and spindle morphology. We cannot rule out the possibility that other substrate interactions contribute to the observed *acm1*Δ phenotypes. However, our data suggest that a primary function of Acm1 might be to specifically limit the interaction between Cdh1 and Hsl1 to late mitosis.

Although loss of *ACM1* in the context of mutant genetic backgrounds has demonstrated that Acm1 can contribute to inhibition of APC^{Cdh1} activity,[11,32] this property appears dispensable for normal cell division, at least under laboratory conditions. Our results provide a satisfying explanation for the apparent redundancy in Cdh1 inhibitory mechanisms and justify the conservation of Acm1 during budding yeast evolution. Cdk phosphorylation inhibits the Cdh1-APC interaction[5] but does not appear to influence D and KEN box-based substrate binding to Cdh1.[7,10] Acm1, on the other hand, is insufficient on its own for complete inactivation of APC^{Cdh1} but is an effective competitive inhibitor of at least some Cdh1-substrate interactions. The two mechanisms therefore appear to serve different and complementary purposes.

Multiple pathways contribute to correct positioning of the nucleus and spindle.[13] One pathway is dependent on cytoplasmic dynein, and our results demonstrating a synthetic genetic interaction between Dyn1 and Acm1 argue that Cdh1 targets influencing nuclear position are likely not components of this pathway. The Hsl1 kinase, a well-established component of the yeast morphogenesis checkpoint that regulates Swe1 levels[33] and resides at the bud neck,[30] has not previously been implicated in nuclear positioning during cell division. However, the bud neck is an important platform for cytoplasmic microtubule interactions during nuclear positioning,[34] and our results clearly link the Cdh1-Hsl1 interaction at the bud neck to the *acm1*Δ phenotype.

Although localization of Cdh1 to the bud neck was first observed nearly a decade ago,[31] the biological importance of this localization remains unknown. Several Cdh1 substrates also localize to the bud neck, including the Swe1 regulators Hsl1, Clb2 and Cdc5 [35] and the IQGAP protein Iqg1, which plays an essential role in cytokinesis.[36] The degradation of Swe1 itself may be at least partially APC-dependent.[37] Thus, one possibility is that following Acm1 degradation initiated in early anaphase,[8,9,12] Cdh1 is recruited to the bud neck via the high affinity interaction with its substrate Hsl1. This specific localization could then allow the rapid, efficient and coordinated clearance of several key Cdh1 substrates once APC^{Cdh1} is activated by the mitotic exit network and Cdc14-catalyzed Cdh1 dephosphorylation.[38,39] It is important to note that the premature interaction between Cdh1 and Hsl1 at the bud neck in the absence of Acm1 does not, by itself, lead to Hsl1 degradation (**Fig. 3**). Thus, the inactive state of Cdh1 is apparently fully maintained by Cdk phosphorylation until mitotic exit in *acm1*Δ cells.

Although our data suggest a role for Hsl1 in correct nuclear positioning, the mechanism by which it might act is not apparent from this study. A direct role, which could be inhibited when Cdh1 is inappropriately bound, is one possibility. Alternatively, the effect of the Cdh1-Hsl1 interaction on nuclear position could simply be an indirect consequence of prematurely recruiting Cdh1 to the bud neck. The presence of Cdh1 could disrupt the function or regulation of another protein or the ability of Hsl1 to bind and recruit another protein that contributes to nuclear position at the bud neck. Further studies will be required to understand the mechanisms by which nuclear position and spindle morphology are perturbed in *acm1*Δ cells and the roles that Hsl1 might play.

Our results reveal that APC coactivators can engage substrates and disrupt their normal function even in the absence of APC activity. In budding yeast, one consequence of Acm1 loss may be genome instability due to generation of multinucleate cells (**Fig. 2**). Loss of Cdh1 function in yeast and human cells results in genome instability, and Cdh1 haploinsufficiency predisposes mice to cancer.[3,40,41] We found that *cdh1*Δ cells exhibited a mild spindle morphology defect (compared with *acm1*Δ cells) and an increase in binucleate cells, consistent with a previous report in reference 15. The fact that similar phenotypes are observed upon either loss of Cdh1 function or failure to properly restrain Cdh1 function highlights the critical role that Cdh1 plays in maintaining genome stability and the requirement for a multifaceted and stringent regulatory system to precisely control Cdh1 expression and activity.

Given the conservation of APC function and mechanism throughout eukaryotes, it is likely that other organisms face a similar challenge of regulating coactivator-substrate interactions. Pseudosubstrates may be a common solution, as several have been identified in diverse organisms.[42-47] The known pseudosubstrates possess no obvious sequence similarity other than the short substrate-like degron motifs, suggesting that they evolved independently. The ability of pseudosubstrates to both inhibit APC^{Cdh1} activity and prevent undesired substrate interactions may explain why they have been favored repeatedly during evolution.

Materials and Methods

Strain and plasmid construction. Yeast plasmids and strains were constructed using standard methods and are listed and described in **Tables S1 and S2**, respectively. All plasmid constructs were confirmed by DNA sequencing and immunoblotting. All strains were confirmed by PCR and, whenever possible, immunoblotting. Additional details are available on request.

Cell growth. Standard yeast growth conditions were used throughout. For microscopy experiments, synthetic selective medium was supplemented with 50 μg/ml adenine. Cultures were arrested in G_1 with 5 μg/ml α factor peptide (Genscript), S with 10 mg/ml hydroxyurea (Sigma), metaphase by adding 2% glucose to P_{GAL1}-*CDC20* strains and late anaphase by shifting *cdc15-2* strains to 37°C. For synchronous release, arrested cells were washed and resuspended in fresh medium at 37°C. Cell cycle stage was monitored by DAPI staining and scoring for DNA segregation. For experiments testing effects of the Hsl1-mdb/mkb mutant, cells were grown in rich medium containing 2% raffinose and 2% galactose at 18°C.

Microscopy. For spindle imaging, cells were collected after > 95% were large budded, fixed in 4% *p*-formaldehyde/4% sucrose for 15 min and washed with phosphate-buffered saline (PBS). For nuclear imaging, cells were fixed with 3.7% formaldehyde for 1 h, washed with PBS, suspended in PBS containing 2 μg/ml DAPI for 5 min and washed extensively with PBS. For Cdh1-EGFP localization experiments, cells were simply washed once with PBS and imaged directly. EGFP was fused to the Cdh1 C terminus to prevent APC^{Cdh1} activity and therefore avoid substrate degradation. This was important particularly in the *acm1*Δ *hsl1*Δ cells, in which expression of active Cdh1 from the *ADH1* promoter is highly toxic.

All images were acquired using a 100x oil immersion lens on an Olympus BX51 microscope equipped with a Hamamatsu Orca-R^2 digital camera and MetaMorph software (Molecular Devices). Confocal microscopy was performed on a Nikon A1R inverted microscope with NIS-elements software. Z-stacks were assembled from 0.4 μm slices ranging between 2 μm above and below the cells. Brightness and contrast were adjusted equally for all images within a figure using ImageJ (NIH).

For quantification of spindle morphology, only large budded cells with no re-budding were considered. Spindles were categorized as normal only if continuous and mostly linear fluorescence signal was observed stretching between both cell poles. Slight deviations from the primary spindle axis less than two times the average spindle width were allowed. Breaks in signal near the bud neck were common and were allowed if the two visible spindle halves were collinear along the mother-bud axis. For quantification of nuclear division, only large budded cells with clearly segregated DNA masses were included.

Immunoblotting. Immunoblotting was performed with the following antibodies: anti-HA 12CA5 (0.4 μg/ml) and anti-myc 9E10 (0.4 μg/ml) were from Roche Applied Science; rabbit anti-Clb2 (0.2 μg/ml) and goat anti-Cdc5 (0.8 μg/ml) were from Santa Cruz Biotechnology; custom rabbit anti-Acm1 raised against recombinant Acm1 was generated by Pacific Immunology,

purified using a GST-Acm1 affinity column and used at 0.04 μg/ml; rabbit anti-G6PD (0.2 μg/ml) and anti-FLAG M2 (0.1 μg/ml) were from Sigma Aldrich.

Affinity purification and mass spectrometry. Cdh1-C/IR and the Cdh1 WD40 domain[7] were expressed with N-terminal 3xFLAG/6His and 3xFLAG fusions, respectively, from P_{GAL1} on a CEN plasmid in strain YKA268 (*acm1*Δ *cdh1*Δ) by addition of 2% galactose for 2 h at 30°C. Cells were lysed by blending with 0.5 mm glass beads on ice in buffer C (50 mM sodium phosphate (pH 7.5), 100 mM NaCl, 10% glycerol and 0.1% Triton X-100) supplemented with 5 mM EDTA, 1 mM PMSF, 1 μM pepstatin and 100 μM leupeptin. Extracts were clarified by centrifugation and the soluble fractions incubated with 50 μl EZView anti-FLAG M2 affinity resin (Sigma) for 2 h at 4°C. The resin was washed with buffer C and bound proteins eluted by incubation with 250 μg/ml 3xFLAG peptide (Sigma) in buffer C for 20 min at room temp. For Cdh1-C/IR, eluted proteins were then incubated with 50 μl EZView Ni^{+2} affinity resin (Sigma) for 1 h at 4°C. The resin was washed with buffer C and bound proteins eluted with buffer C containing 250 mM imidazole. For both fusions, eluted proteins were separated by SDS-PAGE with Coomassie blue staining and entire lanes, including control samples, were excised and cut into 12 slices. Proteins were processed for mass spectral analysis from the gel slices as described in reference 10. Peptides from each sample were separated on Zorbax C_{18} trap and analytical capillary columns (Agilent) with a gradient of increasing acetonitrile (5–40%) in 0.1% formic acid at 300 nl/min on an Agilent 1100 nanoHPLC system. Eluted peptides were injected into an LTQ-Orbitrap XL mass spectrometer (Thermo Scientific) with a nanoelectrospray source. The Orbitrap was operated in data-dependent tandem MS mode with cycles of one MS scan followed by 10 MS/MS scans. MS/MS spectra were searched against a database of *S. cerevisiae* proteins using Sorcerer (Sage-N Research) and Mascot (Matrix Science) search engines. We only report protein hits with at least three matched peptides in the experimental sample, 0 matched peptides in the corresponding control sample and a Mascot protein score greater than 100.

Disclosure of Potential Conflicts of Interest

No potential conflicts of interest were disclosed.

Acknowledgments

This work was supported by NSF grant MCB 0841748 to M.C.H. The Purdue Research Foundation provided support to J.S.M. We thank Kerry Bloom and Jeff Moore for comments and suggestions. We thank Janet Burton and Mark Solomon for providing the *cdh1-D12* and *hsl1-mdb/mkb* mutants and communicating results prior to publication. We thank Dr. Aaron Taylor of the Bindley Bioscience Imaging Facility for assistance with the confocal microscopy.

Note

Supplemental material can be found at:
www.landesbioscience.com/journals/cc/article/18945

References

1. Barford D. Structure, function and mechanism of the anaphase promoting complex (APC/C). Q Rev Biophys 2011; 44:153-90; PMID:21092369; http://dx.doi.org/10.1017/S0033583510000259.
2. Peters JM. The anaphase promoting complex/cyclosome: a machine designed to destroy. Nat Rev Mol Cell Biol 2006; 7:644-56; PMID:16896351; http://dx.doi.org/10.1038/nrm1988.
3. García-Higuera I, Manchado E, Dubus P, Canamero M, Mendez J, Moreno S, et al. Genomic stability and tumour suppression by the APC/C cofactor Cdh1. Nat Cell Biol 2008; 10:802-11; PMID:18552834; http://dx.doi.org/10.1038/ncb1742.
4. Lehman NL, Tibshirani R, Hsu JY, Natkunam Y, Harris BT, West RB, et al. Oncogenic regulators and substrates of the anaphase promoting complex/cyclosome are frequently overexpressed in malignant tumors. Am J Pathol 2007; 170:1793-805; PMID:17456782; http://dx.doi.org/10.2353/ajpath.2007.060767.
5. Zachariae W, Schwab M, Nasmyth K, Seufert W. Control of cyclin ubiquitination by CDK-regulated binding of Hct1 to the anaphase promoting complex. Science 1998; 282:1721-4; PMID:9831566; http://dx.doi.org/10.1126/science.282.5394.1721.
6. Kramer ER, Scheuringer N, Podtelejnikov AV, Mann M, Peters JM. Mitotic regulation of the APC activator proteins CDC20 and CDH1. Mol Biol Cell 2000; 11:1555-69; PMID:10793135.
7. Choi E, Dial JM, Jeong DE, Hall MC. Unique D box and KEN box sequences limit ubiquitination of Acm1 and promote pseudosubstrate inhibition of the anaphase-promoting complex. J Biol Chem 2008; 283:23701-10; PMID:18596038; http://dx.doi.org/10.1074/jbc.M803695200.
8. Enquist-Newman M, Sullivan M, Morgan DO. Modulation of the mitotic regulatory network by APC-dependent destruction of the Cdh1 inhibitor Acm1. Mol Cell 2008; 30:437-46; PMID:18498748; http://dx.doi.org/10.1016/j.molcel.2008.04.004.
9. Ostapenko D, Burton JL, Wang R, Solomon MJ. Pseudosubstrate inhibition of the anaphase-promoting complex by Acm1: regulation by proteolysis and Cdc28 phosphorylation. Mol Cell Biol 2008; 28:4653-64; PMID:18519589; http://dx.doi.org/10.1128/MCB.00055-08.
10. Martinez JS, Jeong DE, Choi E, Billings BM, Hall MC. Acm1 is a negative regulator of the Cdh1-dependent anaphase-promoting complex/cyclosome in budding yeast. Mol Cell Biol 2006; 26:9162-76; PMID:17030612; http://dx.doi.org/10.1128/MCB.00603-06.
11. Robbins JA, Cross FR. Requirements and reasons for effective inhibition of the anaphase promoting complex activator CDH1. Mol Biol Cell 2010; 21:914-25; PMID:20089834; http://dx.doi.org/10.1091/mbc.E09-10-0901.
12. Hall MC, Jeong DE, Henderson JT, Choi E, Bremmer SC, Iliuk AB, et al. Cdc28 and Cdc14 Control Stability of the Anaphase-promoting Complex Inhibitor Acm1. J Biol Chem 2008; 283:10396-407; PMID:18287090; http://dx.doi.org/10.1074/jbc.M710011200.
13. Moore JK, Cooper JA. Coordinating mitosis with cell polarity: Molecular motors at the cell cortex. Semin Cell Dev Biol 2010; 21:283-9; PMID:20109571; http://dx.doi.org/10.1016/j.semcdb.2010.01.020.
14. Yeh E, Skibbens RV, Cheng JW, Salmon ED, Bloom K. Spindle dynamics and cell cycle regulation of dynein in the budding yeast, *Saccharomyces cerevisiae*. J Cell Biol 1995; 130:687-700; PMID:7622568; http://dx.doi.org/10.1083/jcb.130.3.687.
15. Bartholomew CR, Woo SH, Chung YS, Jones C, Hardy CF. Cdc5 interacts with the Wee1 kinase in budding yeast. Mol Cell Biol 2001; 21:4949-59; PMID:11438652; http://dx.doi.org/10.1128/MCB.21.15.4949-59.2001.
16. Benanti JA, Matyskiela ME, Morgan DO, Toczyski DP. Functionally distinct isoforms of Cik1 are differentially regulated by APC/C-mediated proteolysis. Mol Cell 2009; 33:581-90; PMID:19285942; http://dx.doi.org/10.1016/j.molcel.2009.01.032.
17. Juang YL, Huang J, Peters JM, McLaughlin ME, Tai CY, Pellman D. APC-mediated proteolysis of Ase1 and the morphogenesis of the mitotic spindle. Science 1997; 275:1311-4; PMID:9036857; http://dx.doi.org/10.1126/science.275.5304.1311.
18. Woodbury EL, Morgan DO. Cdk and APC activities limit the spindle-stabilizing function of Fin1 to anaphase. Nat Cell Biol 2007; 9:106-12; PMID:17173039; http://dx.doi.org/10.1038/ncb1523.
19. Schwab M, Lutum AS, Seufert W. Yeast Hct1 is a regulator of Clb2 cyclin proteolysis. Cell 1997; 90:683-93; PMID:9288748; http://dx.doi.org/10.1016/S0092-8674(00)80529-2.
20. Charles JF, Jaspersen SL, Tinker-Kulberg RL, Hwang L, Szidon A, Morgan DO. The Polo-related kinase Cdc5 activates and is destroyed by the mitotic cyclin destruction machinery in *S. cerevisiae*. Curr Biol 1998; 8:497-507; PMID:9560342; http://dx.doi.org/10.1016/S0960-9822(98)70201-5.
21. Burton JL, Solomon MJ. Hsl1p, a Swe1p inhibitor, is degraded via the anaphase-promoting complex. Mol Cell Biol 2000; 20:4614-25; PMID:10848588; http://dx.doi.org/10.1128/MCB.20.13.4614-25.2000.
22. Dial JM, Petrotchenko EV, Borchers CH. Inhibition of APC^{Cdh1} activity by Cdh1/Acm1/Bmh1 ternary complex formation. J Biol Chem 2007; 282:5237-48; PMID:17178718; http://dx.doi.org/10.1074/jbc.M606589200.

23. Yeong FM, Lim HH, Padmashree CG, Surana U. Exit from mitosis in budding yeast: biphasic inactivation of the Cdc28-Clb2 mitotic kinase and the role of Cdc20. Mol Cell 2000; 5:501-11; PMID:10882135; http://dx.doi.org/10.1016/S1097-2765(00)80444-X.
24. Schwab M, Neutzner M, Mocker D, Seufert W. Yeast Hct1 recognizes the mitotic cyclin Clb2 and other substrates of the ubiquitin ligase APC. EMBO J 2001; 20:5165-75; PMID:11566880; http://dx.doi.org/10.1093/emboj/20.18.5165.
25. Vodermaier HC, Gieffers C, Maurer-Stroh S, Eisenhaber F, Peters JM. TPR subunits of the anaphase-promoting complex mediate binding to the activator protein CDH1. Curr Biol 2003; 13:1459-68; PMID:12956947; http://dx.doi.org/10.1016/S0960-9822(03)00581-5.
26. Kraft C, Vodermaier HC, Maurer-Stroh S, Eisenhaber F, Peters JM. The WD40 propeller domain of Cdh1 functions as a destruction box receptor for APC/C substrates. Mol Cell 2005; 18:543-53; PMID:15916961; http://dx.doi.org/10.1016/j.molcel.2005.04.023.
27. Burton JL, Tsakraklides V, Solomon MJ. Assembly of an APC-Cdh1 substrate complex is stimulated by engagement of a destruction box. Mol Cell 2005; 18:533-42; PMID:15916960; http://dx.doi.org/10.1016/j.molcel.2005.04.022.
28. Burton JL, Xiong Y, Solomon MJ. Mechanisms of pseudosubstrate inhibition of the anaphase promoting complex by Acm1. EMBO J 2011; 30:1818-29; PMID:21460798; http://dx.doi.org/10.1038/emboj.2011.90.
29. Burton JL, Solomon MJ. D box and KEN box motifs in budding yeast Hsl1p are required for APC-mediated degradation and direct binding to Cdc20p and Cdh1p. Genes Dev 2001; 15:2381-95; PMID:11562348; http://dx.doi.org/10.1101/gad.917901.
30. Barral Y, Parra M, Bidlingmaier S, Snyder M. Nim1-related kinases coordinate cell cycle progression with the organization of the peripheral cytoskeleton in yeast. Genes Dev 1999; 13:176-87; PMID:9925642; http://dx.doi.org/10.1101/gad.13.2.176.
31. Jaquenoud M, van Drogen F, Peter M. Cell cycle-dependent nuclear export of Cdh1p may contribute to the inactivation of APC/C(Cdh1). EMBO J 2002; 21:6515-26; PMID:12456658; http://dx.doi.org/10.1093/emboj/cdf634.
32. Crasta K, Lim HH, Giddings TH Jr, Winey M, Surana U. Inactivation of Cdh1 by synergistic action of Cdk1 and polo kinase is necessary for proper assembly of the mitotic spindle. Nat Cell Biol 2008; 10:665-75; PMID:18500339; http://dx.doi.org/10.1038/ncb1729.
33. McMillan JN, Longtine MS, Sia RA, Theesfeld CL, Bardes ES, Pringle JR, et al. The morphogenesis checkpoint in *Saccharomyces cerevisiae*: cell cycle control of Swe1p degradation by Hsl1p and Hsl7p. Mol Cell Biol 1999; 19:6929-39; PMID:10490630.
34. Pearson CG, Bloom K. Dynamic microtubules lead the way for spindle positioning. Nat Rev Mol Cell Biol 2004; 5:481-92; PMID:15173827; http://dx.doi.org/10.1038/nrm1402.
35. McMurray MA, Thorner J. Septins: molecular partitioning and the generation of cellular asymmetry. Cell Div 2009; 4:18; PMID:19709431; http://dx.doi.org/10.1186/1747-1028-4-18.
36. Ko N, Nishihama R, Tully GH, Ostapenko D, Solomon MJ, Morgan DO, et al. Identification of Yeast IQGAP (Iqg1p) as an Anaphase-Promoting-Complex Substrate and Its Role in Actomyosin-Ring-Independent Cytokinesis. Mol Biol Cell 2007; 18:5139-53; PMID:17942599; http://dx.doi.org/10.1091/mbc.E07-05-0509.
37. Thornton BR, Toczyski DP. Securin and B-cyclin/CDK are the only essential targets of the APC. Nat Cell Biol 2003; 5:1090-4; PMID:14634663; http://dx.doi.org/10.1038/ncb1066.
38. Jaspersen SL, Charles JF, Morgan DO. Inhibitory phosphorylation of the APC regulator Hct1 is controlled by the kinase Cdc28 and the phosphatase Cdc14. Curr Biol 1999; 9:227-36; PMID:10074450; http://dx.doi.org/10.1016/S0960-9822(99)80111-0.
39. Visintin R, Craig K, Hwang ES, Prinz S, Tyers M, Amon A. The phosphatase Cdc14 triggers mitotic exit by reversal of Cdk-dependent phosphorylation. Mol Cell 1998; 2:709-18; PMID:9885559; http://dx.doi.org/10.1016/S1097-2765(00)80286-5.
40. Ross KE, Cohen-Fix O. The role of Cdh1p in maintaining genomic stability in budding yeast. Genetics 2003; 165:489-503; PMID:14573464.
41. Engelbert D, Schnerch D, Baumgarten A, Wasch R. The ubiquitin ligase APC(Cdh1) is required to maintain genome integrity in primary human cells. Oncogene 2008; 27:907-17; PMID:17700535; http://dx.doi.org/10.1038/sj.onc.1210703.
42. Miller JJ, Summers MK, Hansen DV, Nachury MV, Lehman NL, Loktev A, et al. Emi1 stably binds and inhibits the anaphase-promoting complex/cyclosome as a pseudosubstrate inhibitor. Genes Dev 2006; 20:2410-20; PMID:16921029; http://dx.doi.org/10.1101/gad.1454006.
43. Hsu JY, Reimann JD, Sorensen CS, Lukas J, Jackson PK. E2F-dependent accumulation of hEmi1 regulates S phase entry by inhibiting APC(Cdh1). Nat Cell Biol 2002; 4:358-66; PMID:11988738; http://dx.doi.org/10.1038/ncb785.
44. Burton JL, Solomon MJ. Mad3p, a pseudosubstrate inhibitor of APC^{Cdc20} in the spindle assembly checkpoint. Genes Dev 2007; 21:655-67; PMID:17369399; http://dx.doi.org/10.1101/gad.1511107.
45. Malureanu LA, Jeganathan KB, Hamada M, Wasilewski L, Davenport J, van Deursen JM. BubR1 N Terminus Acts as a Soluble Inhibitor of Cyclin B Degradation by APC/CCdc20 in Interphase. Dev Cell 2009; 16:118-31; PMID:19154723; http://dx.doi.org/10.1016/j.devcel.2008.11.004.
46. Kimata Y, Kitamura K, Fenner N, Yamano H. Mes1 controls the meiosis I to meiosis II transition by distinctly regulating APC/C co-activators Fzr1/Mfr1 and Slp1 in fission yeast. Mol Biol Cell 2011; 22:1486-94; PMID:21389117; http://dx.doi.org/10.1091/mbc.E10-09-0774.
47. Kimata Y, Trickey M, Izawa D, Gannon J, Yamamoto M, Yamano H. A mutual inhibition between APC/C and its substrate Mes1 required for meiotic progression in fission yeast. Dev Cell 2008; 14:446-54; PMID:18331722; http://dx.doi.org/10.1016/j.devcel.2007.12.010.